

The Effect of Process Models on Short-term Prediction of Moving Objects for Unmanned Ground Vehicles

R. Madhavan and C. Schlenoff

Abstract—We are developing a novel framework, PRIDE (PRediction In Dynamic Environments), to perform moving object prediction for unmanned ground vehicles. The underlying concept is based upon a multi-resolutional, hierarchical approach which incorporates multiple prediction algorithms into a single, unifying framework. The lower levels of the framework utilize estimation-theoretic short-term predictions while the upper levels utilize a probabilistic prediction approach based on situation recognition with an underlying cost model. The estimation-theoretic short-term prediction is via an extended Kalman filter-based algorithm using sensor data to predict the future location of moving objects with an associated confidence measure. The proposed estimation-theoretic approach does not incorporate *a priori* knowledge such as road networks and traffic signage and assumes uninfluenced constant trajectory and is thus suited for short-term prediction in both on-road and off-road driving.

In this paper, we analyze the complementary role played by vehicle kinematic models in such short-term prediction of moving objects. In particular, the importance of vehicle process models and their effect on predicting the position and orientation of moving objects for unmanned ground vehicle navigation are examined in this paper. We present results using field data obtained from different unmanned ground vehicles operating in a variety of unstructured and unknown environments.

Index Terms—unmanned ground vehicles, estimation theory, moving object prediction.

I. INTRODUCTION

Successful and purposive navigation of unmanned ground vehicles in unstructured and unknown environments demands the competency of the vehicle to predict, with an associated level of confidence, the future locations of moving objects that could interfere with its path. Although the emphasis of this paper is on vehicles, moving objects are not restricted to solely falling within this category. Examples of moving objects that the unmanned vehicle may encounter include other vehicles, people, or animals. We are using the 4D/RCS (Real-Time Control System) reference model architecture [1] as the basis in which to apply the representational approaches that are being developed in this effort. 4D/RCS was chosen due to its explicit and well-defined world modeling capabilities and interfaces, as well as its multi-resolution, hierarchical planning approach.

Commercial equipment and materials are identified in this paper in order to adequately specify certain procedures. Such identification does not imply recommendation or endorsement by the National Institute of Standards and Technology, nor does it imply that the materials or equipment identified are necessarily the best available for the purpose.

The authors are with the Intelligent Systems Division, National Institute of Standards and Technology, Gaithersburg, MD 20899-8230, U.S.A. {raj.madhavan, craig.schlenoff}@nist.gov

Specifically, 4D/RCS allows for planning at multiple levels of abstraction, using different planning approaches as well as utilizing inherently different world model representation requirements. By applying this architecture, we can ensure that the representations being developed for representing moving objects can accommodate different types of planners that have different representational requirements.

The RCS architecture supports multiple behavior generation (BG) systems working cooperatively to compute a final plan for the autonomous system. The spatial and temporal resolution of the individual BG systems along with the amount of time allowed for each BG system to compute a solution are specified by the level of the architecture where it resides. In addition to multiple BG systems, multiple world models are supported with each world model's content being tailored to the systems that it supports (in this case the BG system). As such, it is necessary for moving objects to be represented differently at the different levels of the architecture.

To support this requirement, we have developed the PRIDE (PRediction In Dynamic Environments) framework. The underlying concept is based upon a multi-resolutional, hierarchical approach that incorporates multiple prediction algorithms into a single, unifying framework. This framework supports the prediction of the future location of moving objects at various levels of resolution, thus providing prediction information at the frequency and level of abstraction necessary for planners at different levels within the hierarchy. To date, two prediction approaches have been applied to this framework.

At the higher levels of the framework, moving object prediction may occur at a much lower frequency and a greater level of inaccuracy is tolerable. At these levels, moving objects are identified as far as the sensors can detect, and a determination is made as to which objects should be classified as "objects of interest". In this context, an object of interest is an object that has a possibility of affecting our path in the time horizon in which we are planning. At the lower levels, we utilize estimation-theoretic short-term predictions via an Extended Kalman Filter (EKF) algorithm using sensor data to predict the future location of moving objects with an associated confidence measure.

Once objects of interest are identified, we use a moving object prediction approach based on situation recognition and probabilistic prediction algorithms to predict where we expect that object to be at various time steps into the future. Situation recognition is performed using spatio-temporal reasoning and pattern matching with an *a priori* database

of situations that are expected to be encountered in the environment. A description of this approach is beyond the scope of this paper. More details can be found in [4]. In these algorithms, we are typically looking at planning horizons on the order of tens of seconds into the future with plan steps at about one second intervals. At this level, we are not looking to predict the exact location of the moving object. Instead, we are attempting to characterize the types of actions we expect the moving object to take and the approximate location the moving object would be in if it took that action. Active research is exploring the integration of these two prediction approaches in a way that the predictions from one can help to enforce the predictions of the other or vice-versa.

In this paper, we concentrate on estimation-theoretic short-term predictions of moving objects by analyzing the complementary role played by vehicle process models. In particular, the importance of vehicle kinematic models and their effect on predicting the position and orientation of moving objects for unmanned ground vehicle navigation are examined using both simulated and real field data.

The paper is structured as follows: Section II details how short-term prediction of moving objects is performed within the PRIDE framework. Section III describes the development of vehicle process models and discusses their effects for estimating the position of a 4WD vehicle. Section IV presents experimental and simulation results of the developed vehicle models followed by conclusions in Section V.

II. SHORT-TERM PREDICTION OF MOVING OBJECTS

As outlined in Section I, the short-term prediction is performed using an EKF-based algorithm utilizing on-board sensor data to predict the future location of moving objects with an associated confidence measure. The proposed estimation-theoretic approach does not incorporate *a priori* knowledge such as road networks and traffic signage and assumes uninfluenced constant trajectory and is thus suited for short-term prediction in both on-road and off-road driving.

The strength of using an EKF is that it provides a covariance matrix that is indicative of the uncertainty in the prediction. An EKF employs a process model to estimate the future location of the object of interest. Since the object classification module provides the type of moving object whose position and orientation needs to be predicted, we have envisaged a bank of EKFs for each type of classified object. In turn, this has the added advantage of cross-corroborating the object classification itself as the uncertainty in the EKF prediction will be an indicator of the quality of the prediction. The higher the uncertainty, the lower the confidence in the selection of the correct set of object models and thus consequently decreasing the confidence of the object classification. Thus, our approach combines low-level (image segmentation/classification) and

mid-level (recursive trajectory estimation) information to obtain the short-term prediction and combines it with the cross-corroboration to work symbiotically to effectively reduce the total uncertainty in predicting the positions and orientations of moving objects.

For short-term predictions, it was found that a separate EKF is necessary for different types of moving objects as opposed to a separate EKF for each individual moving object. In essence, a separate prediction equation is needed when the dynamics of the moving object significantly change. For example, multiple variations of tracked tanks could all use the same prediction equations since the kinematics of these tanks do not differ significantly. However, these equations could not be used for wheeled vehicles. Additionally, a generalized prediction equation was sufficient for near-term planning until the moving object could be classified. In our simulated experiments, classification could be performed within 50 sensor observations. At a typical sensor rate of 30 Hz, this resulted in an initial classification within two seconds. Therefore, a generalized prediction equation was used for the first two seconds until the object was classified, at which point, the object-specific prediction equation was applied.

III. EFFECT OF PROCESS MODELS ON SHORT-TERM PREDICTION

This section develops kinematic vehicle models for a 4WD vehicle by accounting for variables enabling the sufficient capture of vehicle motion that is key to short-term moving object prediction.

A. Process Models for a Four-Wheel-Drive Vehicle

The model geometry of the four-wheel-drive (4WD) vehicle is shown in Figure 1. The vehicle states include the cartesian position (x_v, y_v) centered mid-way between the rear wheels and the orientation, ϕ_v of the vehicle. V is the measured velocity of the rear wheels, V' is the velocity of the front wheels along the steered angle γ and B is the vehicle wheel-base.

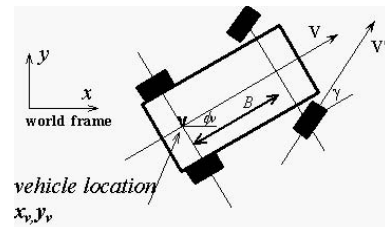


Fig. 1. Process model geometry for the 4WD vehicle.

The continuous model of the vehicle with all quantities referenced to the center of the rear axle of the vehicle can be written using the relation $V'(t) = \frac{V(t)}{\cos \phi_v(t)}$ as:

$$\begin{aligned} \dot{x}_v(t) &= V(t) \cos \phi_v(t) \\ \dot{y}_v(t) &= V(t) \sin \phi_v(t) \\ \dot{\phi}_v(t) &= \left[\frac{1}{B} \right] V(t) \tan \gamma(t) \end{aligned} \quad (1)$$

B. Accounting for Wheel Slip

When a significant amount of wheel slip is present, the shaft velocity encoder measurements are no longer representative of the vehicle speed but in turn are indicative of the wheel speed. So a wheel radius state, r_v , is introduced in addition to the vehicle pose states. The wheel radius is modeled as a discrete additive disturbance rate error (a random walk) such that the error is the integral of white noise. Although in practice this variable may not evolve in a strictly Brownian manner, the Brownian model reflects the growth in uncertainty in its true value and the rate at which the true value is considered to vary. Wheel radius changes are a function of tire pressures, loading effects, temperature, wear and tear and vehicle dynamics.

The velocity measured by the shaft encoder may be replaced by the product of the wheel radius and the wheel angular speed so that $V(t) = r_v(t)\omega(t)$. The control signals applied to the vehicle are: $\mathbf{u}_k = [\omega_k, \gamma_k]$ where ω_k is the angular velocity and γ_k is the steering angle of the 4WD vehicle at time instant k . By integrating using Euler approximation and assuming that the control signals, ω and γ , are approximately constant over the sample period, the nominal discrete process model equations at time instant k can be written as:

$$\begin{pmatrix} x_{v_k} \\ y_{v_k} \\ \phi_{v_k} \\ r_{v_k} \end{pmatrix} = \begin{pmatrix} x_{v_{k-1}} \\ y_{v_{k-1}} \\ \phi_{v_{k-1}} \\ r_{v_{k-1}} \end{pmatrix} + \Delta T \begin{pmatrix} \omega_k r_{v_{k-1}} \cos \phi_{v_{k-1}} \\ \omega_k r_{v_{k-1}} \sin \phi_{v_{k-1}} \\ \left[\frac{1}{B}\right] \omega_k r_{v_{k-1}} \tan \gamma_k \\ \delta r_{v_{k-1}} \end{pmatrix} \quad (2)$$

where ΔT is the synchronous sampling interval between states at discrete time instants, $(k-1)$ and k .

The errors due to the control inputs ω and γ are modeled as simple additive noise sources, $\delta\omega$ and $\delta\gamma$ about their respective means $\bar{\omega}$ and $\bar{\gamma}$ as below:

$$\omega_k = \bar{\omega}_k + \delta\omega_k; \quad \gamma_k = \bar{\gamma}_k + \delta\gamma_k$$

The error source vector due to both modeling errors and uncertainty in control is now defined as:

$$\delta\mathbf{w}_k = [\delta\omega_k, \delta\gamma_k, \delta r_{v_k}]^T$$

where T denotes matrix transposition. The source errors $\delta\omega$, $\delta\gamma$ and δr_v are assumed to be zero-mean, uncorrelated Gaussian sequences with constant variances σ_ω^2 , σ_γ^2 and $\sigma_{r_v}^2$, respectively.

C. Estimation Cycle for the 4WD Vehicle

To formulate a Kalman filter algorithm, process and observation (measurement) models are needed [3]. In view of the availability of data at discrete instants of time from asynchronous sensors and implementation based on digital computers, a discrete time formulation of the continuous time vehicle kinematic models are necessary. In discrete time, only discrete sampling instants t_0, t_1, \dots are considered. The discrete time process model is usually derived by integrating the continuous time process model between

two consecutive time steps. A general discrete time process model can be expressed as

$$\mathbf{x}_k = \mathbf{f}(\mathbf{x}_{k-1}, \mathbf{u}_k, k) + \mathbf{w}_k \quad (3)$$

where $\mathbf{f}(\cdot, \cdot, k)$ is a discrete function that maps the previous state and control inputs to the current state, \mathbf{x}_k is the state at time instant k , \mathbf{u}_k is a known control vector, and \mathbf{w}_k is the discrete process noise.

Observations of the state \mathbf{x}_k are made according to the observation model:

$$\mathbf{z}_k = \mathbf{h}(\mathbf{x}_k, k) + \mathbf{v}_k \quad (4)$$

where $\mathbf{h}(\cdot, k)$ is the discrete function that maps the current state to observations.

The process noise, \mathbf{w}_k and the measurement noise \mathbf{v}_k are assumed to be a Gaussian-distributed random variable of zero mean with covariances \mathbf{Q}_k and \mathbf{R}_k , respectively, and are written as¹:

$$\begin{aligned} \mathbf{w}_k &\sim \mathcal{N}(\mathbf{0}, \mathbf{Q}_k); & \mathbf{E}[\mathbf{w}_k] &= \mathbf{0} \quad \forall k \\ \mathbf{v}_k &\sim \mathcal{N}(\mathbf{0}, \mathbf{R}_k); & \mathbf{E}[\mathbf{v}_k] &= \mathbf{0} \quad \forall k \end{aligned}$$

where $\mathbf{E}[\cdot]$ is the mathematical expectation operator.

In an autonomous vehicle navigation context, the prediction stage uses a model of the motion of the vehicle (a process model having the form described in Equation (3)) to predict the vehicle position, $\hat{\mathbf{x}}_{(k|k-1)}$, at instant k given the information available until and including instant $(k-1)$. The state prediction function $\mathbf{f}(\cdot)$ is defined by Equation (3) assuming zero process and control noise. The prediction of state is therefore obtained by simply substituting the previous state and current control inputs into the state transition equation with no noise. Taking expected values of Equation (2) conditioned on the first $(k-1)$ observations, the state prediction of the EKF becomes:

$$\begin{pmatrix} x_{v_{(k|k-1)}} \\ y_{v_{(k|k-1)}} \\ \phi_{v_{(k|k-1)}} \\ r_{v_{(k|k-1)}} \end{pmatrix} = \begin{pmatrix} x_{v_{(k-1|k-1)}} \\ y_{v_{(k-1|k-1)}} \\ \phi_{v_{(k-1|k-1)}} \\ r_{v_{(k-1|k-1)}} \end{pmatrix} + \Delta T \begin{pmatrix} \omega_k r_{v_{(k-1|k-1)}} \cos \phi_{v_{(k-1|k-1)}} \\ \omega_k r_{v_{(k-1|k-1)}} \sin \phi_{v_{(k-1|k-1)}} \\ \left[\frac{1}{B}\right] \omega_k r_{v_{(k-1|k-1)}} \tan \gamma_k \\ 0 \end{pmatrix}$$

The prediction covariance can now be computed using the Equation:

$$\mathbf{P}_{(k|k-1)} = \nabla \mathbf{f}_{\mathbf{x}_{v_k}} \mathbf{P}_{(k-1|k-1)} \nabla \mathbf{f}_{\mathbf{x}_{v_k}}^T + \nabla \mathbf{f}_{\mathbf{w}_k} \Sigma_c \nabla \mathbf{f}_{\mathbf{w}_k}^T$$

where $\nabla \mathbf{f}_{\mathbf{x}_{v_k}}$ represents the Jacobian evaluated with respect to the states, $\nabla \mathbf{f}_{\mathbf{w}_k}$ is the Jacobian with respect to the error

¹The notation $\mathbf{x} \sim \mathcal{N}(\mathbf{m}, \mathbf{P})$ indicates that \mathbf{x} is a Gaussian (normal) random vector with mean \mathbf{m} and covariance \mathbf{P} .

sources and Σ_c is the noise strength matrix given by:

$$\begin{aligned}\nabla \mathbf{f}_{\mathbf{x}_{v_k}} &= \begin{bmatrix} 1 & 0 & -\Delta T \omega_k r_{v_{k-1}} \sin \phi_{v_{k-1}} & \Delta T \omega_k \cos \phi_{v_{k-1}} \\ 0 & 1 & \Delta T \omega_k r_{v_{k-1}} \cos \phi_{v_{k-1}} & \Delta T \omega_k \sin \phi_{v_{k-1}} \\ 0 & 0 & 1 & \Delta T \left[\frac{1}{B} \right] \omega_k \tan \gamma_k \\ 0 & 0 & 0 & 1 \end{bmatrix} \\ \nabla \mathbf{f}_{\mathbf{w}_k} &= \Delta T \begin{bmatrix} r_{v_{k-1}} \cos \phi_{v_{k-1}} & 0 & 0 & 0 \\ r_{v_{k-1}} \sin \phi_{v_{k-1}} & 0 & 0 & 0 \\ \left[\frac{1}{B} \right] r_{v_{k-1}} \tan \gamma_k & \left[\frac{1}{B} \right] \omega_k r_{v_{k-1}} (1 + \tan^2 \gamma_k) & 0 & 0 \\ 0 & 0 & 0 & 1 \end{bmatrix} \\ \Sigma_c &= \begin{bmatrix} \sigma_\omega^2 & 0 & 0 \\ 0 & \sigma_\gamma^2 & 0 \\ 0 & 0 & \sigma_{r_v}^2 \end{bmatrix}\end{aligned}$$

When an exteroceptive sensor observation becomes available, the states of the EKF (comprising of the moving object's position and orientation) are to be updated so that during the next cycle the prediction starts from a reasonably known position. This is important since the EKF computes the future position based on the current position. If the prediction starts from a wrong position, the cumulative errors will result in an estimate that will be far from the truth.

Once the state and covariance predictions are available, the next step is to compute a predicted observation and a corresponding innovation for updating the predicted state. Expanding Equation (4) as a Taylor series about the predicted state $\hat{\mathbf{x}}_{(k|k-1)}$

$$\hat{\mathbf{z}}_k = \mathbf{h}(\hat{\mathbf{x}}_{(k|k-1)}, \mathbf{u}_k, k) + \nabla \mathbf{h}_{\mathbf{x}_k} [\hat{\mathbf{x}}_{(k|k-1)} - \mathbf{x}_k] + O([\hat{\mathbf{x}}_{(k|k-1)} - \mathbf{x}_k]^2) + \mathbf{v}_k$$

where $\nabla \mathbf{h}_{\mathbf{x}_k}$ is the Jacobian evaluated at $\mathbf{x}_k = \hat{\mathbf{x}}_{(k|k-1)}$. The predicted observation $\hat{\mathbf{z}}_{(k|k-1)}$ is found by using the non-linear relation described in Equation (4) and taking expectations conditioned on the first $(k-1)$ observations by considering only terms up to the first order and neglecting higher order terms such that

$$\hat{\mathbf{z}}_{(k|k-1)} \triangleq \mathbb{E}[\mathbf{z}_k | \mathbf{Z}_{k-1}] = \mathbf{h}(\hat{\mathbf{x}}_{(k|k-1)})$$

The difference between the actual observation and the predicted observation at time step k is termed the innovation and is written as: $\nu_k = \mathbf{z}_k - \hat{\mathbf{z}}_{(k|k-1)}$. The innovation covariance is found by squaring the estimated observation error and taking expectations conditioned on the first $(k-1)$ measurements

$$\mathbf{S}_k = \nabla \mathbf{h}_{\mathbf{x}_k} \mathbf{P}_{(k|k-1)} \nabla \mathbf{h}_{\mathbf{x}_k}^T + \mathbf{R}_k$$

The observations that arrive are accepted only if the observation falls inside the normalized innovation validation gate, $\nu_k^T \mathbf{S}_k^{-1} \nu_k \leq \epsilon_\gamma$, where ν_k is the innovation defined as the difference between the actual and predicted positions. The value of ϵ_γ can be chosen from the fact that the normalized innovation sequence is a χ^2 random variable with m degrees of freedom (m being the dimension of the observation) [3].

Once a validated observation is available, the update of the estimate equal to the weighted sum of the observation and the prediction can be computed as:

$$\hat{\mathbf{x}}_{(k|k)} = \hat{\mathbf{x}}_{(k|k-1)} + \mathbf{W}_k \nu_k$$

where \mathbf{W}_k is the Kalman gain matrix determined by the relative confidence in vehicle prediction and observation and determines the influence of the innovation on the updated estimate. The error in the updated estimate is

$$\begin{aligned}\tilde{\mathbf{x}}_{(k|k)} &= \mathbf{x}_k - \hat{\mathbf{x}}_{(k|k)} \\ &= \mathbf{x}_k - [\hat{\mathbf{x}}_{(k|k-1)} + \mathbf{W}_k \nu_k] = \tilde{\mathbf{x}}_{(k|k-1)} - \mathbf{W}_k \nu_k\end{aligned}$$

The covariance update is

$$\mathbf{P}_{(k|k)} = \mathbb{E}[\tilde{\mathbf{x}}_{(k|k)} \tilde{\mathbf{x}}_{(k|k)}^T] = \mathbf{P}_{(k|k-1)} - \mathbf{W}_k \mathbf{S}_k \mathbf{W}_k^T$$

where the Kalman gain matrix is given by

$$\mathbf{W}_k = \mathbf{P}_{(k|k-1)} \nabla \mathbf{h}_{\mathbf{x}_k}^T \mathbf{S}_k^{-1}$$

D. Accounting for Wheel Slip and Skid

To account for both slip and skid of the vehicle that might be present, two states V_s and γ_s can be added to the process model. The errors in slip and skid of the vehicle are modeled as discrete random walks such that they are the integral of white noise and are found to provide better performance.

The control signals applied to the vehicle in this case are $\mathbf{u}_k = [V_k, \gamma_k]$ where V_k and γ_k are the speed and steering angle of the 4WD vehicle, respectively. The nominal discrete process model equations at time instant k can now be written as:

$$\begin{pmatrix} x_{v_k} \\ y_{v_k} \\ \phi_{v_k} \\ V_{s_k} \\ \gamma_{s_k} \end{pmatrix} = \begin{pmatrix} x_{v_{k-1}} \\ y_{v_{k-1}} \\ \phi_{v_{k-1}} \\ V_{s_{k-1}} \\ \gamma_{s_{k-1}} \end{pmatrix} + \Delta T \begin{pmatrix} (V_k + V_{s_{k-1}}) \cos \phi_{v_{k-1}} \\ (V_k + V_{s_{k-1}}) \sin \phi_{v_{k-1}} \\ \frac{1}{B} (V_k + V_{s_{k-1}}) \tan(\gamma_k + \gamma_{s_{k-1}}) \\ \delta V_{s_{k-1}} \\ \delta \gamma_{s_{k-1}} \end{pmatrix}$$

The errors due to the control inputs V and γ are modeled as simple additive noise sources, δV and $\delta \gamma$ about their respective means \bar{V} and $\bar{\gamma}$ as below:

$$V_k = \bar{V}_k + \delta V_k; \quad \gamma_k = \bar{\gamma}_k + \delta \gamma_k$$

The error source vector is defined as:

$$\delta \mathbf{w}_k = [\delta V_k, \delta \gamma_k, \delta V_{s_k}, \delta \gamma_{s_k}]^T$$

The source errors δV , $\delta \gamma$, δV_s and $\delta \gamma_s$ are assumed to be zero-mean, uncorrelated Gaussian sequences with constant variances σ_V^2 , σ_γ^2 , $\sigma_{V_s}^2$ and $\sigma_{\gamma_s}^2$, respectively.

Additionally, the vehicle position estimates (x_v, y_v) are correlated with the vehicle orientation (ϕ_v) estimates; errors as a result of the orientation cause errors in the vehicle position estimates. When the steering rate is high, the orientation error is also at its highest and the position subsequently becomes highly correlated with the orientation estimates. The addition of the Σ_s matrix helps to decorrelate the effects of orientation on the position estimates of the vehicle. The Jacobians and the stabilizing noise matrix are as given below:

$$\nabla \mathbf{f}_{\mathbf{x}_{v_k}} = \begin{bmatrix} 1 & 0 & -\Delta T k_1 \sin \phi_{v_{k-1}} & \Delta T \cos \phi_{v_{k-1}} & 0 \\ 0 & 1 & \Delta T k_1 \cos \phi_{v_{k-1}} & \Delta T \sin \phi_{v_{k-1}} & 0 \\ 0 & 0 & 1 & \Delta T \frac{1}{B} \tan k_2 & \Delta T \frac{k_1}{B} (1 + \tan^2 k_2) \\ 0 & 0 & 0 & 1 & 0 \\ 0 & 0 & 0 & 0 & 1 \end{bmatrix}$$

$$\nabla f_{w_k} = \begin{bmatrix} \Delta T \cos \phi_{v_{k-1}} & 0 & 0 & 0 \\ \Delta T \sin \phi_{v_{k-1}} & 0 & 0 & 0 \\ \Delta T \frac{1}{B} \tan k_2 & \Delta T \frac{k_1}{B} (1 + \tan^2 k_2) & 0 & 0 \\ 0 & 0 & \Delta T & 0 \end{bmatrix}$$

$$\Sigma_c = \begin{bmatrix} \sigma_V^2 & 0 & 0 & 0 \\ 0 & \sigma_\gamma^2 & 0 & 0 \\ 0 & 0 & \sigma_{V_s}^2 & 0 \\ 0 & 0 & 0 & \sigma_{\gamma_s}^2 \end{bmatrix}$$

$$\Sigma_s = \begin{bmatrix} \frac{\sigma_V^2}{10^2} & 0 & 0 & 0 \\ 0 & \frac{\sigma_\gamma^2}{10^2} & 0 & 0 \\ 0 & 0 & \frac{\sigma_{V_s}^2}{10^3} & 0 \\ 0 & 0 & 0 & \frac{(\sigma_V^2 + \sigma_\gamma^2 + \sigma_{V_s}^2 + \sigma_{\gamma_s}^2)}{10^7} \end{bmatrix}$$

where $k_1 \triangleq V_k + V_{s_{k-1}}$
 $k_2 \triangleq \gamma_k + \gamma_{s_{k-1}}$

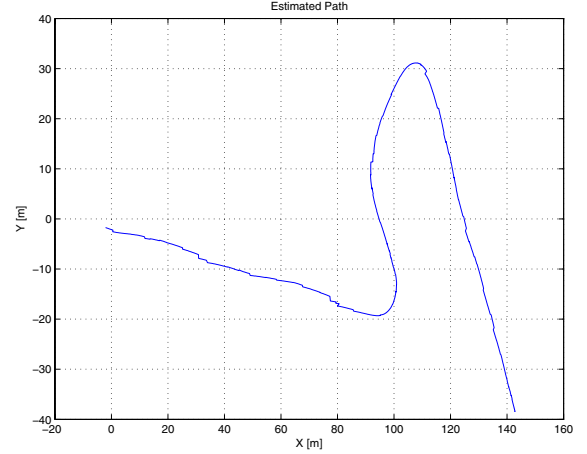
IV. EXPERIMENTAL RESULTS AND DISCUSSION

To validate the process models, we present results using both simulated and real field data. The simulation data was obtained using a Distributed Interactive Simulation (DIS) platform namely Modular Semi Automated Forces (ModSAF), a training and research system developed by the U.S. Army's Program Executive Office for Simulation, Training, and Instrumentation Command. Typically, ModSAF models are employed to represent individual soldiers or vehicles and their coordination into orderly-moving squads and platoons; but, their tactical actions as units are planned and executed by a human controller. ModSAF uses state transition constructs inspired by finite state machines (FSMs) to represent the behavior and functionality of a process for a pre-defined number of states. By querying ModSAF, we can retrieve an object's location at any given time.

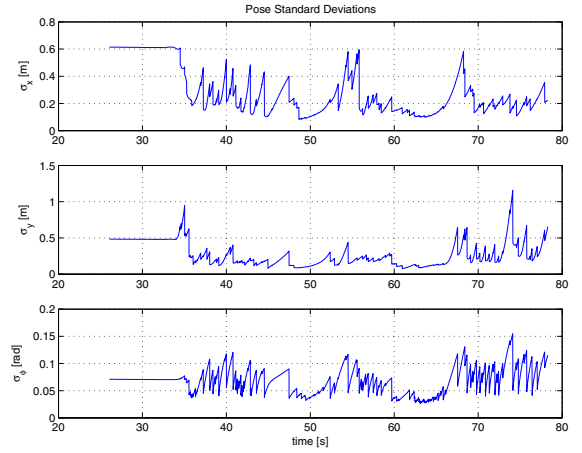
The real field data was logged as the 4WD vehicle traversed unstructured and undulating terrain. This vehicle was equipped with a bearing-only laser and wheel and steering encoders. External corrections were provided using observations from landmarks in the environments that were detected by the bearing-only laser. For additional details, see [2].

Figure 2(a) shows the estimated path of the 4WD vehicle using the process model that accounts for both vehicle slip and skid. The exclusion of the slip and skid variables in addition to the stabilizing noise matrix would result in the predicted vehicle path drifting and the error growing without bounds. This is easy to understand as the estimated vehicle position at a given instant depends on the previous estimate which makes it difficult to eliminate errors associated with the previous cycle due to sensor inaccuracies, the assumption that the heading remains constant over the sampling interval, wheel slippage and quantization effects. As a consequence, the vehicle pose (position and especially the orientation) would become less and less certain and the errors associated with the pose grow without bound.

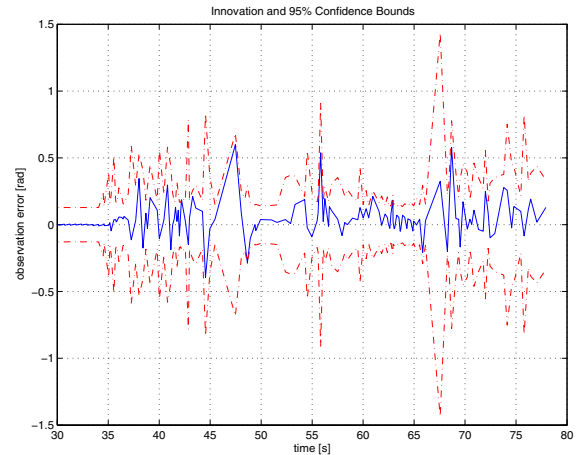
In Figure 2(b), the periodic rise and fall of the pose standard deviations can be seen. The decrease in the standard



(a)



(b)



(c)

Fig. 2. (a), (b) and (c) show the predicted path, the pose standard deviations and the innovation with 95% confidence bounds (dotted line), respectively. In (a), the starting location of the vehicle is at (142.76, -38.31). The direction of travel is from right to left.

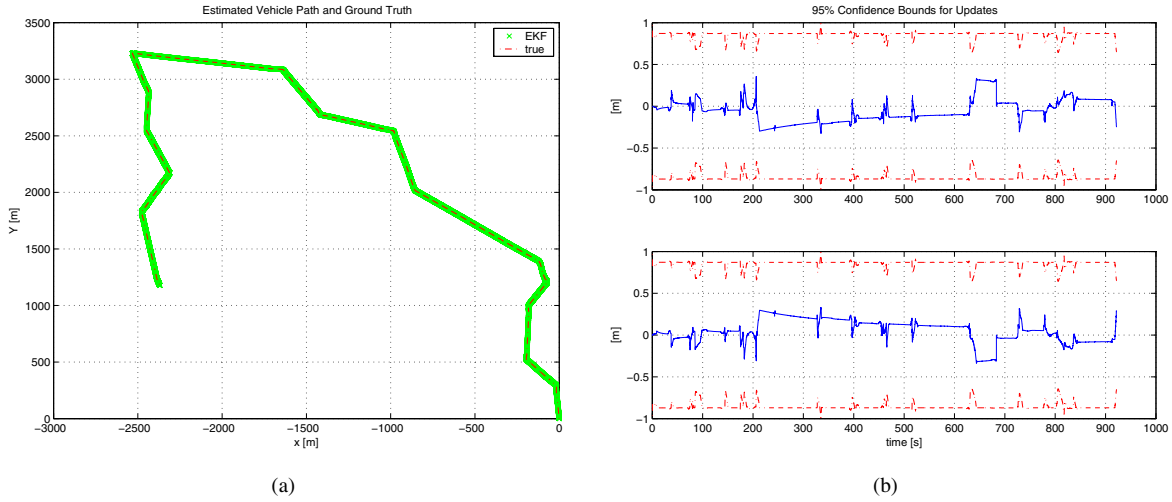


Fig. 3. (a), and (b) show the predicted path, the errors in position between the predicted path and the ground truth with 95% confidence bounds (dotted line), respectively. The traverse is approximately 7 kms long and takes about 15 minutes of simulation time to travel at a speed of 8 m/s. The updates were generated at a rate of 15 Hz.

deviations is due to certain landmarks coming into view and being detected reliably. The increase in standard deviations is due to the vehicle moving away from the landmarks and its position being estimated based on the prediction alone. When the landmarks provide no aiding information towards estimating the pose of the vehicle, the standard deviation is at a maximum. Thus the algorithm continually corrects the diverging dead-reckoning estimates based on external sensing information provided by the landmarks (also see Figure 2(a)). The bearing-only laser innovation sequence along with the 95% (2σ) bounds is shown in Figure 2(c). Due to the observation validation procedure, the innovations are clearly bounded.

Figure 3 depicts the results obtained using data from the simulation platform. Here, we are able to generate *ground truth* to compare the predicted position estimates generated by a vehicle model of the form shown in Equation (2). The position of the vehicle is predicted until the errors exceed a predefined threshold. Once the errors are above a given threshold, an update is deemed to be performed by utilizing the observations from ModSAF. We check the validity of the observation by testing if it falls within the normalized innovation gate. A validated observation is then used to update the states of the EKF and the estimation cycle continues as in the 4WD vehicle case.

Figure 3(a) shows the predicted path, and 3(b) the position errors with the 2σ observation confidence bounds, respectively. It can be seen that the predicted path and the ground truth agree well. As before, the validated innovation sequence falls within the prescribed 95% (2σ) bounds indicative of consistent vehicle state estimates.

V. CONCLUSIONS AND FURTHER WORK

In this paper, we analyzed the effect of vehicle process models on the short-term prediction of moving objects within the PRIDE framework. In particular, the importance of vehicle process models and their effect on predicting the position and orientation of moving objects for unmanned ground vehicle navigation was examined using both simulated and real data for a 4WD vehicle operating in different environments. We presented results that showed the need for sufficiently adequate process models and their importance in short-term moving object prediction.

As we move forward with the PRIDE framework, many issues remain to be addressed. The short-term predictions, as discussed in this paper, will need to be quantitatively compared to the longer-term predictions being determined at the higher levels of the architecture. In addition, the short-term predictions may be used as inputs to the longer-term prediction to better refine the estimates. We also plan to investigate the applicability of other prediction algorithms such as particle filters within the architecture.

REFERENCES

- [1] J. Albus et al. 4D/RCS Version 2.0: A Reference Model Architecture for Unmanned Vehicle Systems. Technical Report NISTIR 6910, National Institute of Standards and Technology, Gaithersburg, MD 20899, U.S.A., 2002.
- [2] R. Madhavan and H. Durrant-Whyte. Terrain Aided Localization of Autonomous Ground Vehicles. *Journal of Automation in Construction (Invited)*, 13(1):69–86, January 2004.
- [3] P. Maybeck. *Stochastic Models, Estimation, and Control Vol. 1*. Academic Press, New York, June 1979.
- [4] C. Schlenoff, R. Madhavan, and T. Barbera. A Hierarchical, Multi-Resolutional Moving Object Prediction Approach for Autonomous On-Road Driving. In *Proceedings of the IEEE Intl. Conf. on Robotics and Automation*, pages 1956–1961, April 2004.